

## Research Article

# The Effect of Water on the Tin Electrodeposition from [Bmim]HSO<sub>4</sub> Ionic Liquid

Jie Tang , DongLiang Lv, CunYing Xu , YiXin Hua, QiBo Zhang, PingZhao Niu, and XiaoLin Zhu

*Department of Metallurgical and Energy Engineering, Kunming University of Science and Technology, Kunming 650093, China*

Correspondence should be addressed to CunYing Xu; [xucunying@foxmail.com](mailto:xucunying@foxmail.com)

Received 24 March 2018; Revised 12 July 2018; Accepted 19 July 2018; Published 9 August 2018

Academic Editor: Davood Nematollahi

Copyright © 2018 Jie Tang et al. This is an open access article distributed under the Creative Commons Attribution License, which permits unrestricted use, distribution, and reproduction in any medium, provided the original work is properly cited.

The electrodeposition of tin from SnO in ionic liquid 1-butyl-3-methylimidazolium hydrogen sulfate ([Bmim]HSO<sub>4</sub>) in the presence of water at different cathodic potential was investigated. With the addition of water to [Bmim]HSO<sub>4</sub> ionic liquid, the electrochemical window of the electrolyte decreases and the reduction potential of Sn(II) positively shifts. The water content of ionic liquid electrolyte has a distinct effect on morphology of the deposits. As water content increased from 0 to 50% (v/v), the morphology of deposits varies from granular to hexagonal rod-like, then to hollow tubular, and finally to wire-like. The XRD phase analysis showed that both Sn and CuSn alloys were deposited in ionic liquid/water mixtures. However, in dried ionic liquids only Cu<sub>3</sub>Sn was obtained, surprisingly. The difference in the structure might be attributed to the various interactions of the ions with the Cu substrate. In addition, the deposition potential was found to play a significant role in the morphology of deposits.

## 1. Introduction

The electrochemical deposition of tin and its alloys is of great practical importance and widely used in the semiconductor industry and field of energy storage devices [1–4], like lithium ion batteries; e.g., traditional electrodeposition of tin and its alloy is performed in aqueous electrolytes including sulfate, fluoborate, and citrate [5–7]. Such electrolytes are susceptible to complex electrolyte composition and quite corrosive and can possibly have a negative impact on the environment. Therefore, it is of interest to find alternative electrolytes for tin deposition.

In recent years, the electrodeposition of metals and alloys from ionic liquids has attracted significant attention. Compared with aqueous solutions, ionic liquids have some unique properties such as negligible vapor pressures, good thermal stability, acceptable electrical conductivity, and wide electrochemical windows [8, 9]. In aqueous solutions the electrodeposition of tin and its alloys is usually accompanied by decomposition of organic additives and often low current efficiencies. Problems associated with organic additives can be avoided by employing ionic liquids because they can be used as electrolyte without any additives. For example, many

metals like Au, Pt, and Cu and their alloys can be prepared in ionic liquids without any side effects [10–13]. Furthermore, the use of ionic liquids as electrolyte might offer environmentally benign conditions compared with conventional aqueous baths.

The electrodeposition of tin has been investigated in some ionic liquids [4, 14], especially AlCl<sub>3</sub>-based ionic liquids [15]. However, this kind of ionic liquid is sensitive to air and water; therefore the experiment must be carried out under inert gas conditions. For this reason, air and water stable ionic liquids were applied for tin electrodeposition [16]. Tachikawa et al. [17] have investigated the electrochemical behaviors of Sn(II)/Sn in 1-n-butyl-1-methylpyrrolidinium bis(trifluoromethylsulfonyl) imide (BMPTFSI). Smooth and dense tin deposits were obtained [17]. Leong et al. [18] have studied the electrodeposition of Sn from 1-ethyl-3-methylimidazolium dicyanamide (EMI-DCA) ionic liquid.

Up to now, most of the work on the electrodeposition of tin in ionic liquids was performed under inert gas conditions in a glove box. Nevertheless, the electrodeposition of tin under air conditions is of considerable interest for industrial production of Sn film and powders. There are no studies focusing on the effect of air and moisture on the deposition of

tin in ionic liquids. In addition, some protic ionic liquids are capable of dissolving various metal oxides, which can be used as electrolytes to recover metals through electrowinning [19]. In the present paper, we focus on the fundamental aspects of tin deposition from SnO in a protic ionic liquids 1-butyl-3-methylimidazolium hydrogen sulfate ([Bmim]HSO<sub>4</sub>) ionic liquid in the presence of water. The influence of water is of interest as in an open bath where would be water uptake in any case.

## 2. Experimental

The ionic liquid [Bmim]HSO<sub>4</sub> was prepared and purified according to the established literature procedures [20]. SnO powder (Aldrich, 99%) was used as a tin source. The dissolution of SnO in [Bmim]HSO<sub>4</sub> was performed in ionic liquid without and with water (10–50%, v/v). The cyclic voltammetry and electrodeposition experiments were carried out in a three electrodes system using an electrochemical workstation (Shanghai Chenhua, CHI760E). The cell was kept closed by a Teflon cap during experiments to avoid the loss of water content via evaporation. The GC electrode (S=0.1256 cm<sup>2</sup>) was used as a working electrode in the cyclic voltammetry measurements. The electrodeposition experiments were conducted on copper substrate (Aldrich, 99%, s=2 cm<sup>2</sup>). A platinum electrode and a silver wire were used as counter and reference electrode, respectively. The reference was directly immersed in the [Bmim]HSO<sub>4</sub> ionic liquid using a separate compartment. The GC working electrode was polished with 0.05 μm alumina paste, rinsed, and dried prior to all measurements. The copper electrode was polished successively with increasingly finer grades of emery paper and finally to a mirror finish with aqueous slurry of 0.05 μm alumina rinsed with distilled water.

After deposition, the samples were rinsed with ethanol to ensure removal of the ionic liquid and subsequently dried under vacuum. The scanning electron microscopy (SEM) associated with energy-dispersive X-ray spectroscopy (EDS) (FCI-quanta-200F) was used to characterize the surface morphology and the composition of the deposits. X-ray diffraction (XRD) analysis was performed using a Siemens D-5000 diffractometer with Cu Kα radiation.

## 3. Results and Discussion

**3.1. Cyclic Voltammetry Analysis.** The cyclic voltammogram recorded at a GC electrode in the [Bmim]HSO<sub>4</sub> containing 40 mM SnO was presented in Figure 1. For comparison, the cyclic voltammogram of [Bmim]HSO<sub>4</sub> ionic liquids on glassy carbon electrodes without and with water is also included in Figure 1. The neat ionic liquid displays a cathodic potential limit of -1.48 V (versus Ag), which results from the reduction of imidazole ion (Bmim<sup>+</sup>) [21]. After the addition of SnO to pure [Bmim]HSO<sub>4</sub> ionic liquid, the new reduction and oxidation waves appear at potentials close to -0.38 V (versus Ag) as a result of the deposition and stripping of Sn. In addition, The second oxidation wave at about 0.46 V corresponds to the oxidation of the Sn(II) ions. When the [Bmim]HSO<sub>4</sub> is mixed with water (30%, v/v), the cathodic

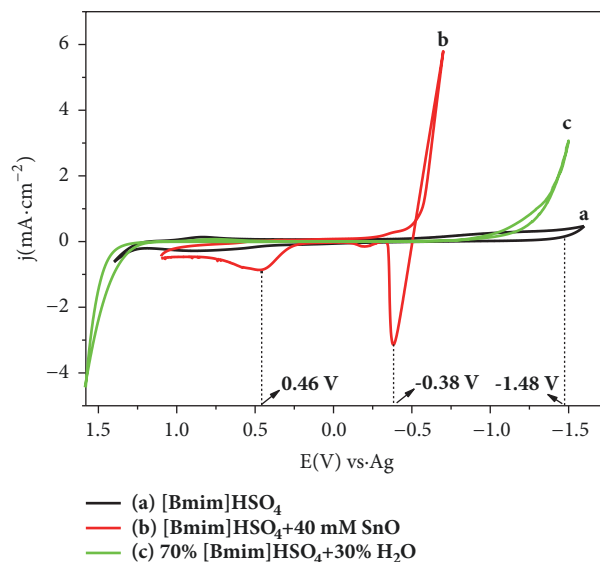


FIGURE 1: Cyclic voltammograms recorded at GC electrode in [Bmim]HSO<sub>4</sub>: (a) pure [Bmim]HSO<sub>4</sub>, (b) [Bmim]HSO<sub>4</sub> containing 40 mM SnO, and (c) [Bmim]HSO<sub>4</sub> containing 30% (v/v) H<sub>2</sub>O. Scan rate: 50 mV/s, 353 K.

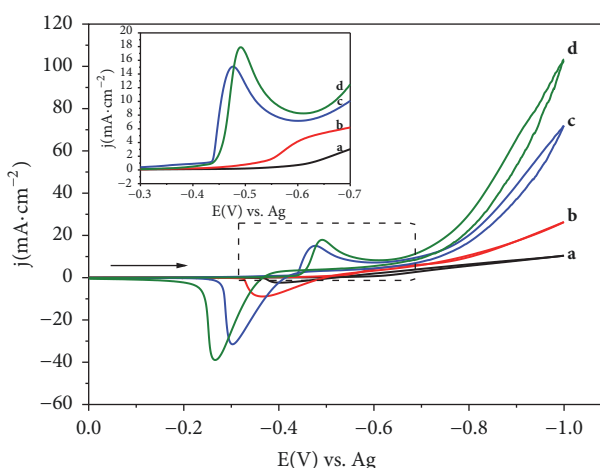


FIGURE 2: Cyclic voltammograms of 40 mM SnO in [Bmim]HSO<sub>4</sub> on GC electrode with different water content and local enlarged image: (a) 0% H<sub>2</sub>O, (b) 10% H<sub>2</sub>O, (c) 30% H<sub>2</sub>O, and (d) 50% H<sub>2</sub>O. Scan rate: 50 mV/s, 353 K.

potential limit of this mixture solution shifts to more positive potential (-0.95 V versus Ag), but far more negative than the reduction potential of Sn(II).

Figure 2 shows the cyclic voltammograms of 40 mM SnO in [Bmim]HSO<sub>4</sub> on glassy carbon electrode with different water contents. With the increase of water content, the initial reduction potential of Sn(II) gradually shifts to more positive potentials, indicating the reduction of Sn(II) becomes easy. The addition of water to the ionic liquid facilitates the decrease in viscosity and a subsequent increase in conductivity. Furthermore, tin ions can be solvated by water to form [Sn(H<sub>2</sub>O)<sub>4</sub>]<sup>2+</sup> rather than being complexed with [HSO<sub>4</sub>]<sup>-</sup>

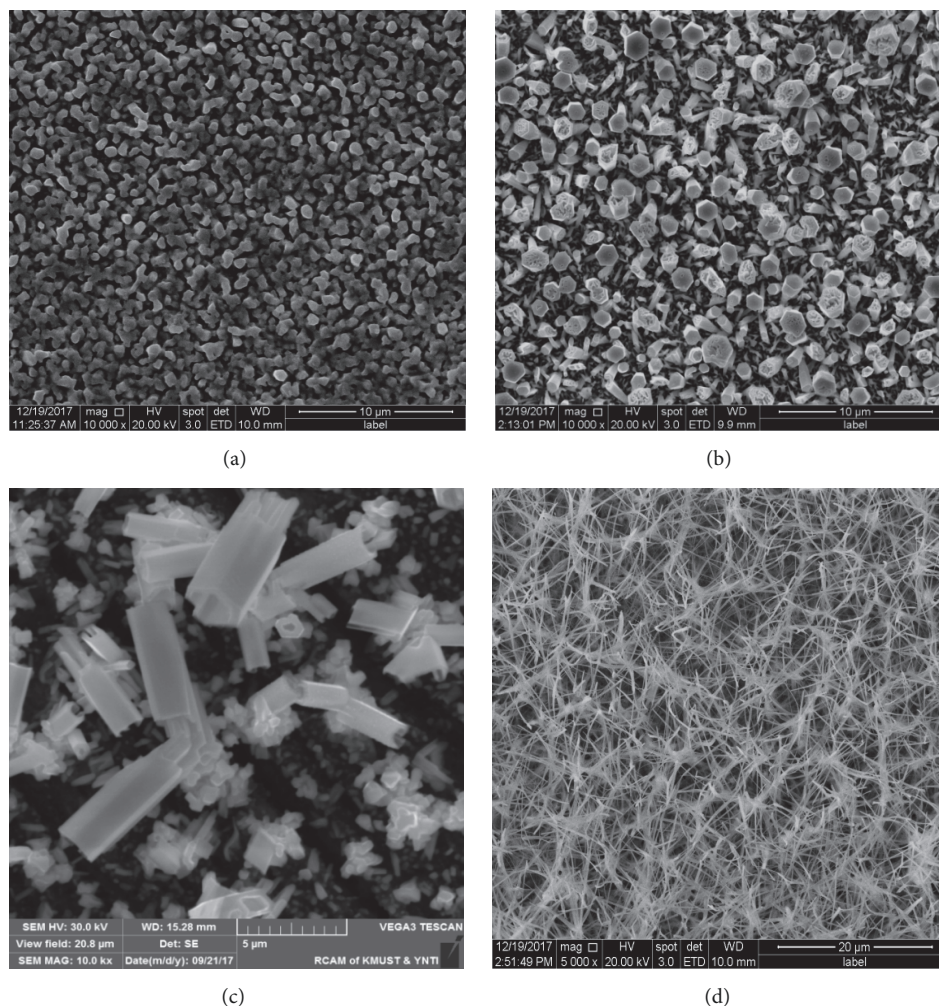


FIGURE 3: SEM images of Sn deposits obtained on Cu substrates from the SnO-[Bmim]HSO<sub>4</sub> solution with different water concentration: (a) 0% H<sub>2</sub>O, (b) 10% H<sub>2</sub>O, (c) 30% H<sub>2</sub>O, and (d) 50% H<sub>2</sub>O. Deposition temperature: 353 K; deposition potential: -0.6 V (versus Ag).

[22]. Compared to the complex ion formed between Sn(II) ions and [HSO<sub>4</sub>]<sup>-</sup>, the smaller size of [Sn(H<sub>2</sub>O)<sub>4</sub>]<sup>2+</sup> ion facilitates diffusion. However, an increase in water content also results in a reduction in the electrochemical window of the ionic liquid. As demonstrated in Figure 2, the electrochemical window is decreased when the water content in the ionic liquids is increased. Similar results were also observed by Compton et al. [23]. It has been reported that the electrochemical window decreases in the following order: vacuum-dried > atmospheric > wet [23]. Furthermore, the CVs shown in Figure 2 reveal higher current densities for Sn deposition/dissolution with increasing water content. With the increasing of water content in electrolyte, the viscosity of electrolyte decreases, and the diffusion rate of Sn(II) ions increases. Thus, in ionic liquid/water mixture the concentration of discharge ions near the cathode is high and the reduction of Sn(II) speeds up.

**3.2. Morphology of Deposits.** The electrodeposition of Sn was carried out in [Bmim]HSO<sub>4</sub> containing 40 mM SnO (SnO-[Bmim]HSO<sub>4</sub>) with different water content at various

deposition potentials (-0.45~-0.60 V versus Ag) and 80°C. This is a suitable temperature for metal electrodeposition in ionic liquids. A large number of our experiments in this work reveal that the thickness and morphology of Sn deposits depend on the deposition time. When the deposition time is less than 2 hours, the resulting deposits are too thin to meet the demand. However, as deposition time exceeds 2 hours, some dendrite crystals begin to emerge on the surface of deposits, and it is easy to fall off by rinsing with water. Thus, the deposition time is selected for 2 hours.

**3.2.1. Effect of the Water Content.** The effect of water on the morphology of the Sn deposits was investigated and the results are shown in Figure 3. As shown in Figure 3(a), The Sn deposits obtained in [Bmim]HSO<sub>4</sub> have a granular morphology with mean grain sizes of about 500 nm. When the [Bmim]HSO<sub>4</sub> electrolyte contains 10% (v/v) water, the deposit is composed of hexagonal prism, and the diameters range from dozens of nm to microlevel. Besides, a fraction of hexagonal prisms has some small holes (Figure 3(b)). With increasing water concentration to 30% (v/v), two types of



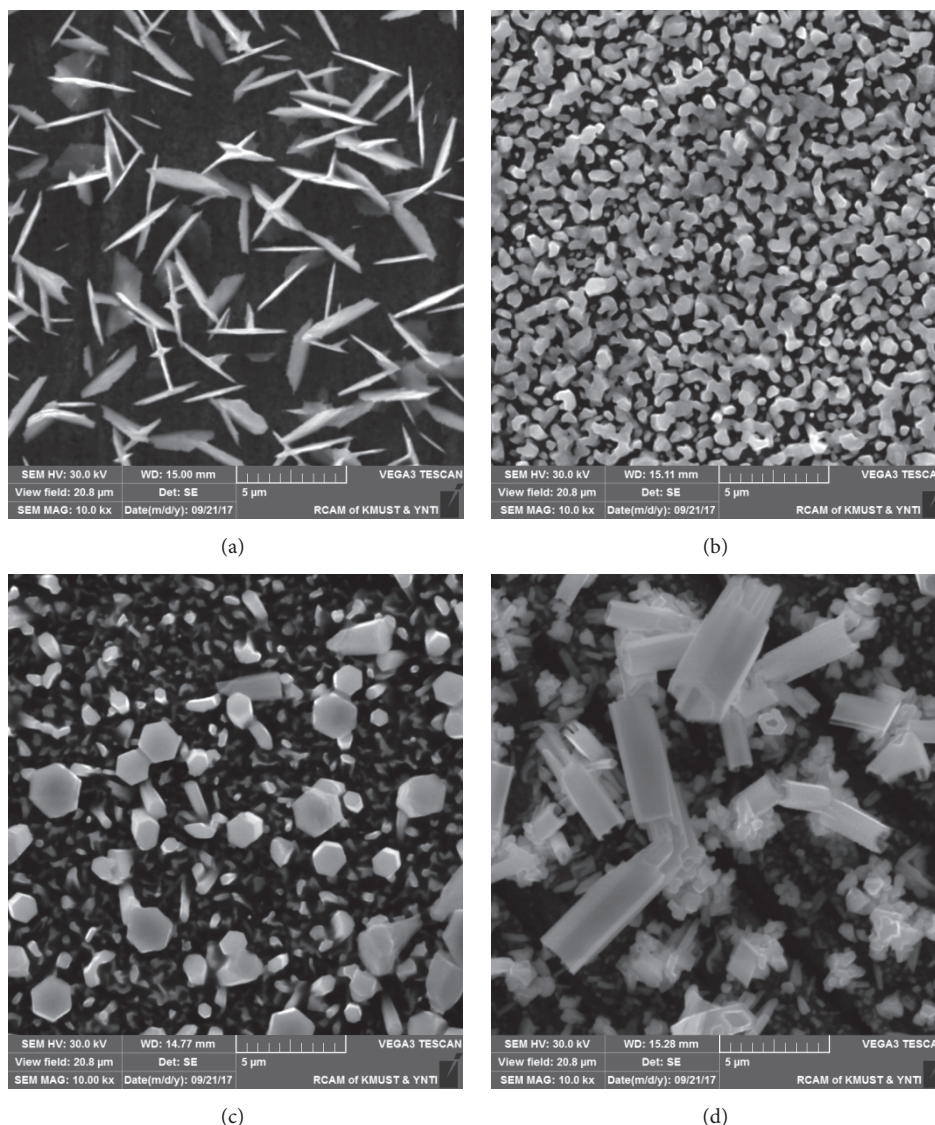


FIGURE 4: SEM images of Sn deposits obtained from the [Bmim]HSO<sub>4</sub>/H<sub>2</sub>O mixture (30% H<sub>2</sub>O, v/v) solution containing 40 mM SnO at different deposition potential: (a) -0.45 V, (b) -0.5 V, (c) -0.55 V, and (d) -0.6 V. Temperature: 353 K.

deposits are formed including hollow tubular and granular, but the dominant shape is hollow tubular (Figure 3(c)). At a higher water concentration of 50% (v/v), disorder tin nanowires with the mean diameter of 70 nm were obtained (Figure 3(d)). Based on the above analysis, the water content of electrolyte has significant influence on the morphology feature. At dried [Bmim]HSO<sub>4</sub>, the electrode surface is covered by imidazole cations, which may hinder the nucleation, crystal growth of certain directions, and surface diffusion process [24]. Therefore, finer tin grain is obtained at dried ionic liquid. The addition of water decreases the solution viscosity and accordingly increases the mass transfer rate of the Sn(II) species as well as the growth rate of the crystal nucleus. In addition, it is interesting to note that the ionic liquid plays a comparable role as surfactant in the ionic liquid/water mixtures. Most solutions used in the electrodeposition of metals contain organic surfactants that have a

specific function in the deposition process [10, 25, 26]. These surfactants affect the nuclei and crystal growth processes as they adsorbed at the surface of the cathode and certain lattice plane. Furthermore, with increasing water content, the effect of ionic liquid as surfactant on the nucleation and crystal growth of products is enhanced during deposition process. It may lead to the formation of hexagonal prism and hollow tubular tin deposits and eventually the formation of disorder nanowires. Consequently, tin deposits in some special morphology can be electrodeposited by controlling water concentration in the SnO-[Bmim]HSO<sub>4</sub> solution.

**3.2.2. Effect of Deposition Potential.** The effect of deposition potential on the morphology of tin deposits obtained in ionic liquid/water mixture (30% H<sub>2</sub>O, v/v) is examined, as shown in Figure 4. It can be seen from Figure 4(d) that hexagonal hollow tubes are obtained at a deposition potential

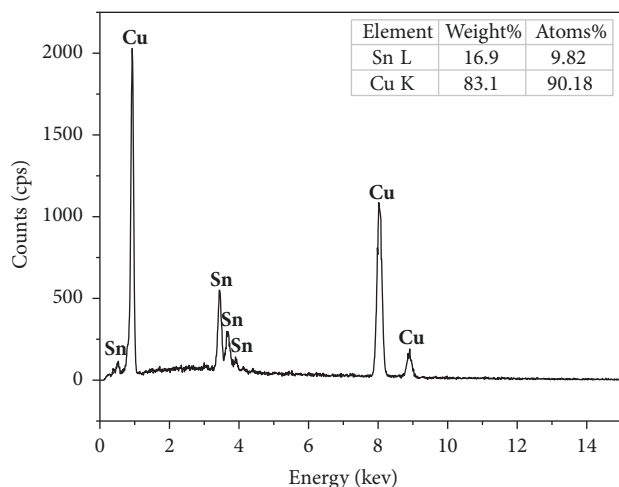


FIGURE 5: EDS spectra of the tin deposits electrodeposited from the [Bmim]HSO<sub>4</sub> ionic liquid containing 40 mM SnO at -0.6 V and 353 K.

of -0.6 V (versus Ag). With the deposition potential positive shift to -0.55 V, hexagonal rods and granules are observed (Figure 4(c)). As electrodeposition of Sn was performed at -0.50 V, the deposit is grainy (Figure 4(b)). The tin deposit obtained at -0.45 V is composed of nanoparticles and some nanoflakes on the surface of nanoparticle layer. These results indicated that decreasing the deposition potential from -0.6 V to -0.45 V leads to the changes in morphologies. At low deposition potentials, the discharge rate of reducible ions on the electrode is lower, and the crystal growth rate is low. With the increasing of deposition potential, however, the crystal growth rate increases. This is in good agreement with the fact that deposits obtained at low deposition potential are smaller size than those obtained at higher deposition potential.

### 3.3. Composition and Phase Structure Analysis

**3.3.1. Effect of Water Content.** The composition of the tin deposits, which were electrodeposited from dried [Bmim]HSO<sub>4</sub> containing 40 mM SnO at -0.6 V, is examined by EDS. The EDS pattern in Figure 5 shows that only tin is present besides the signal from the Cu substrate.

Figure 6 displays the XRD patterns of tin deposits obtained from SnO-[Bmim]HSO<sub>4</sub> without and with water at -0.6 V and 353 K. As shown in Figure 6(a), the diffractogram of the deposits obtained from SnO-[Bmim]HSO<sub>4</sub> contains peaks from Cu<sub>3</sub>Sn alloy and Cu substrate. However, the diffractogram of the deposits obtained from SnO-[Bmim]HSO<sub>4</sub> in the presence of 10% (v/v) water contains not only the characteristic peaks from CuSn alloy, but also the peaks from tin (Figure 6(b)). With increasing the water content of electrolyte to 30% (v/v), the deposits obtained are still composed of Sn and CuSn alloy. The metal tin was found in the deposits obtained from SnO-[Bmim]HSO<sub>4</sub> with water. In addition, the formation of different CuSn alloys was observed in the presence of water. This result shows

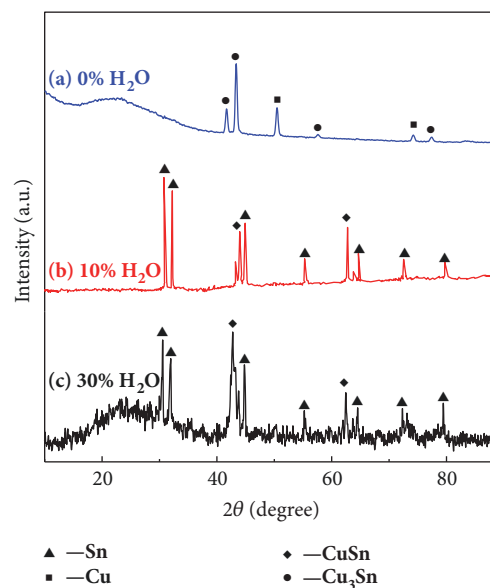


FIGURE 6: XRD patterns of tin deposits obtained from the [Bmim]HSO<sub>4</sub> ionic liquid containing 40 mM SnO with different water content: (a) 0% H<sub>2</sub>O, (b) 10% H<sub>2</sub>O, and (c) 30% H<sub>2</sub>O.

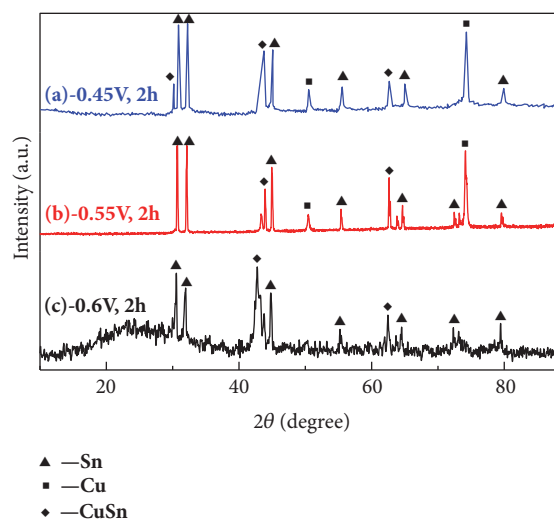


FIGURE 7: XRD patterns of tin deposits obtained from the [Bmim]HSO<sub>4</sub>/H<sub>2</sub>O mixture (30% H<sub>2</sub>O, v/v) solution containing 40 mM SnO at different deposition potential for 2 h. (a) -0.45 V, (b) -0.55 V, and (c) -0.6 V. Temperature: 353 K.

that the interfacial properties and tin growth mechanism are obviously changed in the presence of water.

**3.3.2. Effect of Deposition Potential.** Figure 7 shows that XRD patterns of the deposits obtained from the [Bmim]HSO<sub>4</sub>/H<sub>2</sub>O mixture (30% H<sub>2</sub>O, v/v) solution containing 40 mM SnO at different deposition potential. In the deposition potential range from -0.45 V to -0.60 V, the obtained deposits are the mixtures of Sn and CuSn alloys, indicating that the phase structure of these deposits is independent of the deposition potential. However, the diffraction peaks of the

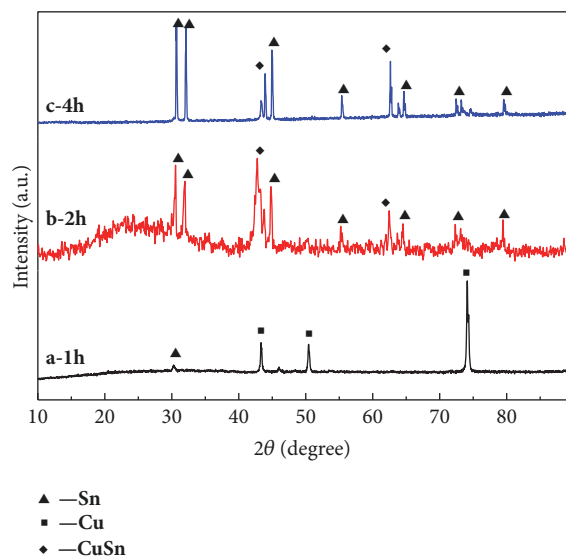


FIGURE 8: XRD patterns of tin deposits obtained from the [Bmim]HSO<sub>4</sub>/H<sub>2</sub>O mixture (30% H<sub>2</sub>O, v/v) solution containing 40 mM SnO at -0.6 V and 353 K for different deposition time: (a) 1 h, (b) 2 h, and (c) 4 h.

copper substrate weaken gradually with the increase of deposition potential. With the deposition potential increasing, the reduction reaction of Sn(II) to Sn speeds up, leading to an increase in the thickness of deposits.

**3.3.3. Effect of Deposition Time.** Figure 8 shows the XRD patterns of tin deposits obtained from the [Bmim]HSO<sub>4</sub>/H<sub>2</sub>O mixture (30% H<sub>2</sub>O, v/v) solution containing 40 mM SnO at different deposition time. The deposit obtained at deposition time of 1 h is very thin. In XRD pattern of this deposit, except for the diffraction peaks of Cu substrate, only very weak diffraction peaks corresponding to Sn are detected. As the deposition time extends to 2 h, not only the diffraction peaks of Sn, but also the peaks of CuSn are observed. With further increasing of deposition time, the intensity of Sn diffraction peaks enhances, while the peaks for CuSn alloy weaken.

For comparison, the electrodeposition of Sn was also conducted on glassy carbon electrode from the [Bmim]HSO<sub>4</sub>/H<sub>2</sub>O mixture (30% H<sub>2</sub>O, v/v) solution containing 40 mM SnO at -0.6 V for 2 h. The sample was examined by XRD, and the result is presented in Figure 9. Unlike on Cu electrode, the XRD result indicates the formation of pure Sn without any hint for the formation of Sn alloy.

## 4. Conclusions

The present paper shows that tin with different morphology and structure can be successfully deposited from [Bmim]HSO<sub>4</sub> ionic liquids in presence of water (10-50%) at different deposition potential. The cyclic voltammograms measured on glassy carbon electrode exhibit a typical redox couple associated with deposition/stripping of tin in the employed electrolyte. The electrochemical window of the ionic liquids decreases with water concentration increasing.

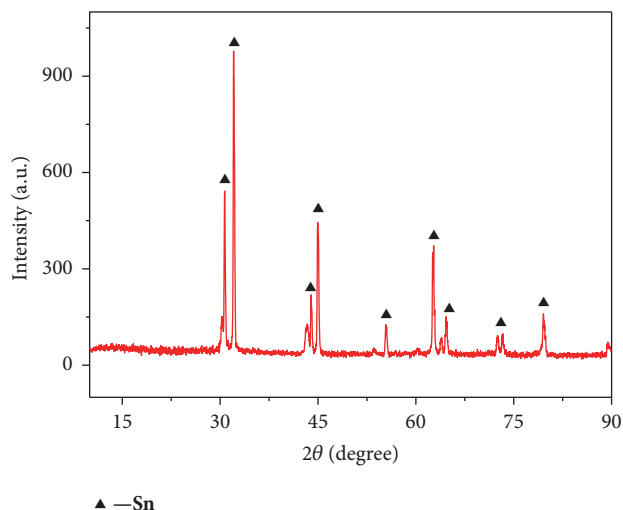


FIGURE 9: XRD patterns of tin deposits obtained on glassy carbon electrode from the [Bmim]HSO<sub>4</sub>/H<sub>2</sub>O mixture (30% H<sub>2</sub>O, v/v) solution containing 40 mM SnO at -0.6 V and 353 K.

Both water and deposition potential have a significant effect on the morphology of the deposits. The different morphologies, including granular, hexagonal rod-like, hollow tubular, wire-like, and flake-like tin powders, are formed. In the presence of water tin and CuSn alloy were formed, whereas, in the pure ionic liquids, only Cu<sub>3</sub>Sn alloys were observed.

## Data Availability

The data used to support the findings of this study are available from the corresponding author upon request.

## Conflicts of Interest

The authors declare that they have no conflicts of interest.

## Authors' Contributions

Jie Tang and DongLiang Lv contributed equally to this work.

## Acknowledgments

This work is supported by the Natural Science Foundation of China (Project no. 51764027).

## References

- [1] M. Li, Y. Yang, Y. Ling et al., "Morphology and Doping Engineering of Sn-Doped Hematite Nanowire Photoanodes," *Nano Letters*, vol. 17, no. 4, pp. 2490–2495, 2017.
- [2] J. L. Martin and M. P. Toben, "Tin and tin-lead alloy electroplating in the electronics industry," *Metal Finishing*, vol. 86, no. 1, pp. 39–41, 1988.
- [3] Y.-G. Guo, J.-S. Hu, and L.-J. Wan, "Nanostructured materials for electrochemical energy conversion and storage devices (*Advanced Materials* (2008) 20 (2878-2887))," *Advanced Materials*, vol. 20, no. 23, pp. 2878–2887, 2008.

- [4] X. Xie, X. Zou, K. Zheng et al., "Ionic liquids electrodeposition of Sn with different structures as anodes for lithium-ion batteries," *Journal of The Electrochemical Society*, vol. 164, no. 14, pp. D945–D953, 2017.
- [5] G. I. Medvedev, L. A. Nekrasova, and N. A. Makrushin, "Tin Electroplating from Sulfate Electrolyte Containing Syntanol, Formalin, and Coumarin," *Russian Journal of Applied Chemistry*, vol. 76, no. 3, pp. 387–390, 2003.
- [6] S. M. Silaimani, M. Pushpavanam, and K. C. Narasimham, "Electrochemical preparation of tin fluoborate for tin plating," *Bulletin of Electrochemistry*, vol. 17, no. 9, pp. 409–414, 2001.
- [7] J.-Y. Lee, J.-W. Kim, B.-Y. Chang, H. T. Kim, and S.-M. Park, "Effects of ethoxylated  $\alpha$ -naphtholsulfonic acid on tin electroplating at iron electrodes," *Journal of The Electrochemical Society*, vol. 151, no. 5, pp. C333–C341, 2004.
- [8] P. Bonhte, A. Dias, N. Papageorgiou, K. Kalyanasundaram, and M. Grätzel, "Hydrophobic, highly conductive ambient-temperature molten salts," *Inorganic Chemistry*, vol. 35, no. 5, pp. 1168–1178, 1996.
- [9] H. Ohno, *Electrochemical Aspects of Ionic Liquids*, John Wiley & Sons, Inc., Hoboken, NJ, USA, 2005.
- [10] F. Endres, M. Bukowski, R. Hempelmann, and H. Natter, "Electrodeposition of nanocrystalline metals and alloys from ionic liquids," *Angewandte Chemie International Edition*, vol. 42, no. 29, pp. 3428–3430, 2003.
- [11] C. Qi, L. Yang, and Y. H. Kang, "Influence of water on active ion in [Bmim]Cl/AlCl<sub>3</sub> ionic liquid," *Journal of Shenyang Normal University*, vol. 34, no. 1, pp. 74–77, 2016.
- [12] Z. Liu, S. Z. E. Abedin, and F. Endres, "Electrodeposition of zinc films from ionic liquids and ionic liquid/water mixtures," *Electrochimica Acta*, vol. 89, pp. 635–643, 2013.
- [13] J. Tang, C. Xu, X. Zhu et al., "Anodic Dissolution of Copper in Choline Chloride-Urea Deep Eutectic Solvent," *Journal of The Electrochemical Society*, vol. 165, no. 9, pp. E406–E411, 2018.
- [14] P. Giridhar, A. M. Elbasiony, S. ZeinElAbedin, and F. Endres, "A Comparative Study on the Electrodeposition of Tin from Two Different Ionic Liquids: Influence of the Anion on the Morphology of the Tin Deposits," *ChemElectroChem*, vol. 1, no. 9, pp. 1549–1556, 2014.
- [15] D. Zhu, H. Sun, and Y. S. Fung, "Electrodeposition of tin from 1-methyl-3-ethylimidazolium chloride/AlCl<sub>3</sub>/SnCl<sub>2</sub> room temperature molten salts," in *Proceedings of the 15th International Symposium on Molten Salts - 210th ECS Meeting*, pp. 239–248, Mexico, November 2006.
- [16] S. Zein El Abedin and F. Endres, "Electrodeposition of metals and semiconductors in air- and water-stable ionic liquids," *ChemPhysChem*, vol. 7, no. 1, pp. 58–61, 2006.
- [17] N. Tachikawa, N. Serizawa, Y. Katayama, and T. Miura, "Electrochemistry of Sn(II)/Sn in a hydrophobic room-temperature ionic liquid," *Electrochimica Acta*, vol. 53, no. 22, pp. 6530–6534, 2008.
- [18] T.-I. Leong, Y.-T. Hsieh, and I.-W. Sun, "Electrochemistry of tin in the 1-ethyl-3-methylimidazolium dicyanamide room temperature ionic liquid," *Electrochimica Acta*, vol. 56, no. 11, pp. 3941–3946, 2011.
- [19] A. P. Abbott, D. L. Davies, G. Capper, R. K. Rasheed, and V. Tambyrajah, *Ionic liquids and their use as solvents*, 2007.
- [20] Y. Zhang, L. I. Jinshi, J. F. Shen, S. H. Yan, and J. W. Liu, "The preparation of [BMIM]HSO<sub>4</sub>/Al<sub>2</sub>O<sub>3</sub> and its use for dehydration of glycerol to acrolein," *Natural Gas Chemical Industry*, vol. 63, no. 2, pp. 109–114, 2012.
- [21] Q.-B. Zhang and Y.-X. Hua, "Effect of the ionic liquid additive-[BMIM]HSO<sub>4</sub> on the kinetics of oxygen evolution during zinc electrowinning," *Wuli Huaxue Xuebao/ Acta Physico - Chimica Sinica*, vol. 27, no. 1, pp. 149–155, 2011.
- [22] D. P. Arnold and J. Blok, "The coordination chemistry of tin porphyrin complexes," *Coordination Chemistry Reviews*, vol. 248, no. 3-4, pp. 299–319, 2004.
- [23] A. M. O'Mahony, D. S. Silvester, L. Aldous, C. Hardacre, and R. G. Compton, "Effect of water on the electrochemical window and potential limits of room-temperature ionic liquids," *Journal of Chemical & Engineering Data*, vol. 53, no. 12, pp. 2884–2891, 2008.
- [24] J. Ru, Y. Hua, C. Xu et al., "Morphology-controlled preparation of lead powders by electrodeposition from different PbO-containing choline chloride-urea deep eutectic solvent," *Applied Surface Science*, vol. 335, pp. 153–159, 2015.
- [25] G. I. Medvedev, N. A. Makrushin, and A. N. Dubenkov, "Electrodeposition of Tin-bismuth Alloy from Sulfate Bath Containing Organic Additives," *Protection of Metals*, vol. 39, no. 4, pp. 381–384, 2003.
- [26] F. Lallemand, L. Ricq, M. Wery, P. Berçot, and J. Pagetti, "The influence of organic additives on the electrodeposition of iron-group metals and binary alloy from sulfate electrolyte," *Applied Surface Science*, vol. 228, no. 1-4, pp. 326–333, 2004.





Hindawi

Submit your manuscripts at  
[www.hindawi.com](http://www.hindawi.com)

